Published in final edited form as:
J Alzheimers Dis. 2018 ; 61(1): 415–424. doi:10.3233/JAD-170344.

Hippocampal Stratum Radiatum, Lacunosum and Moleculare Sparing in Mild Cognitive Impairment

Li Su[#a,b], **Lawrence Hayes**[#a], **Soteris Soteriades**[a], **Guy Williams**[c], **Susannah AE Brain**[d], **Michael J Firbank**[e], **Giulia Longoni**[a], **Robert J Arnold**[a], **James B Rowe**[f,g,+], and **John T O'Brien**[a,+]

[a]Department of Psychiatry, University of Cambridge School of Clinical Medicine, Cambridge, CB2 0SP

[b]China-UK Centre for Cognition and Ageing Research, Faculty of Psychology, Southwest University, Chongqing, China

[c]Wolfson Brain Imaging Centre, University of Cambridge, School of Clinical Medicine, Cambridge Biomedical Campus, Cambridge CB2 0QQ

[d]Oxford University Hospitals NHS Trust, Windmill Road, Oxford OX3 7LD

[e]Institute of Neuroscience and Newcastle University Institute for Ageing, Newcastle University Campus for Ageing and Vitality, Newcastle upon Tyne, NE4 5PL

[f]Department of Clinical Neurosciences, Cambridge University, CB2 0SZ

[g]MRC Cognition and Brain Sciences Unit, Cambridge, CB2 7EF

[#] These authors contributed equally to this work.

Abstract

Background—Alzheimer's disease (AD) is associated with atrophy in entorhinal cortex (ERC), the hippocampus, and its subfields Cornu Ammonis 1 (CA1) and subiculum, which predict conversion from Mild Cognitive Impairment (MCI) to clinical AD. The stratum radiatum, lacunosum and moleculare (SRLM) are also important gateways involving ERC and CA1, which are affected by early AD pathology.

Objective—To assess whether the SRLM is affected in MCI and AD.

Methods—In this proof-of-concept study, 27 controls, 13 subjects with AD and 22 with MCI underwent 3T MRI. T1 maps were used for whole-hippocampal volumetry, T2 maps were

Correspondence to: Dr Li Su, Department of Psychiatry, School of Clinical Medicine, University of Cambridge, Box 189, Level E4, Cambridge Biomedical Campus, Cambridge, UK, CB2 0SP, or China-UK Centre for Cognition and Ageing Research, Faculty of Psychology, Southwest University, Chongqing, China. ls514@cam.ac.uk.
[+]Joint senior authors

Conflict of Interest:
J.T.O. has been a consultant for GE Healthcare, TauRx, Axon, Axovant and Lilly and received honoraria for talks from Piramal.

Description of Author Roles:
L.S. and L.H. co-designed the study, analysed the data and wrote the manuscripts. S.S. analysed part of the data. G.W., M.J.F., S.A.E.B., G.L. and R.J.A. were involved in data collection and analysis and assisted with writing of the manuscript. J.B.R. and J.T.O.co-designed the study, obtained funding for the project and assisted with writing of the manuscript.

Europe PMC Funders Author Manuscripts

segmented for hippocampal subfield areas, entorhinal cortex and subiculum thickness, and evaluated for SRLM integrity.

Results—Significant CA1 atrophy and subiculum thinning were found in both AD and MCI compared to similarly aged controls. However, SRLM integrity was only significantly reduced in AD but not in MCI compared to controls. There were no significant differences in other hippocampal subfields (CA2, CA3/Dentate Gyrus) or ERC thickness between the groups. Finally, CA1 and CA3/DG areas and SRLM clarity were correlated with clinical and cognitive measurements of disease severity.

Conclusion—Although this study was cross sectional, it suggests a progression of specific subfield changes from MCI to established AD that is associated with the reduced integrity of SRLM, which may reflect more widespread hippocampal involvement as the disease progresses and the relative preservation of SRLM in MCI. These results provide new MRI biomarkers for disease staging and understanding of the neurobiology in AD.

Keywords

AD; MCI; dementia; CA1; SRLM; subiculum; hippocampal; subfield; segmentation; MRI

Introduction

Alzheimer's disease (AD) is the commonest cause of neurodegenerative dementia. A subset of patients with Mild Cognitive Impairment (MCI) are increasingly recognised, with symptomatic memory impairment but in whom the criteria for clinical diagnosis of AD are not met. These patients are at heightened risk of conversion to clinical AD, with conversion rate of approximately 10-15% per year compared to 1-2% of comparably aged cognitively normal individuals [1]. For early diagnosis and for monitoring in clinical trials, there is a pressing need for reliable and sensitive biomarkers that span the progression from early MCI to clinical AD.

Brain imaging methods offer potential diagnostic and prognostic biomarkers in MCI and AD, especially where the imaging signals mirror the distribution of neuropathology. For example, numerous neuroimaging studies of AD have demonstrated whole-hippocampal atrophy versus cognitively normal older subjects [2]. However, whole-hippocampal atrophy is also found in other disorders including Parkinson’s disease [3], Dementia with Lewy Bodies (DLB) and vascular dementia [4], potentially limiting its utility as a specific biomarker in differential diagnosis, especially at early stages of MCI.

There is evidence of differential effects of AD pathology among the different hippocampal subfields, with *post mortem* studies showing a hierarchical spread of amyloid and tau pathology beginning in the entorhinal (ERC) and perirhinal cortex, Cornu Ammonis (CA1) subfield and subiculum, and then stratum radiatum, lacunosum and moleculare (SRLM), followed by wider cortical dissemination [5,6]. It has been argued that such propagations are likely driven by transynaptic mechanisms observed from mouse models of AD [6,7] although selective vulnerability may also contribute. Sensitive brain imaging that reflects the

Europe PMC Funders Author Manuscripts

underlying pathology across medial temporal lobe structures would be a significant clinical advance from current whole-hippocampal measures.

The SRLM contains numerous apical dendrites and axonal fasciculi parallel to the internal surface of the Cornu Ammonis, blending with the stratum moleculare of the Dentate Gyrus (DG). The SRLM acts as important gateways with two main glutamatergic excitatory inputs going to CA1 from CA3 and ERC [8], and also have a large population and variety of GABAergic interneurons that play a critical role in modulating the dynamic activity in hippocampus networks [9]. Thus SRLM, which are intimately involved in the pathways between CA1 and CA3/ERC, and between hippocampus and wider cortical areas, are important candidates as biomarkers of MCI and AD.

In an early endeavour using a radial mapping technique on T1-weighted MRI, Apostolova and colleagues reported atrophy of the CA1 region and subiculum in AD [10,11]. An intrinsic limitation of the use of the radial mapping technique is that it only measures changes seen at the surface of the hippocampus, and as such is unable to either directly assess individual subfields or account for changes in deep structures like the DG, SRLM and CA3 subfields, of which a smaller proportion are directly visible on the surface of the hippocampus. Other methods include manual segmentation of high resolution T2 weighted MRI to directly quantify the hippocampal subfields [12,13,14]. Using this technique Mueller and colleagues [12] demonstrated that CA1 atrophy can occur in normal aging, but is markedly increased in AD. These findings are supported by Firbank et al [14] who showed that, in addition to significant CA1 and subiculum atrophy, there was also disproportionate atrophy of the ERC of AD subjects compared to similarly aged controls.

The possibility to detect brain structural changes before AD pathology becomes clinically severe has led to investigation of hippocampal changes in subjects with MCI. Apostolova et al [10] reported that amnestic MCI subjects had atrophy in CA1 and subiculum, albeit less pronounced than in those with AD, and that the degree of atrophy was predictive of conversion to AD [15]. Conversely, Mueller et al [16] showed that it was the CA1 to CA2 transition zone that was atrophied in MCI subjects, and could differentiate MCI from controls. However, due to the variations in analysis techniques and heterogeneity of the samples, it remains unclear from the limited literature to date what is the precise nature of the changes in MCI, how these may change during progression to established AD, and whether they may be potentially useful diagnostic markers at different stages of the disease progression.

We therefore tested the joint hypotheses that MRI can detect greater CA1 and subicular atrophy in AD, compared to controls, and that whilst subjects with MCI have CA1 volume loss, it would be intermediate between the AD and the control groups. Moreover, we predicted that the volume of the other subfields (CA2 and CA3/DG) would be relatively preserved, in both patient groups. Finally we used a visual rating system [14] to score the hypo-intense line within the hippocampus, which represents the highly myelinated fibres in the SRLM, as demonstrated by Coras et al [17], using a combination of ultra high field (7T) MRI and histological technique. We hypothesised that this imaging marker may demonstrate

Europe PMC Funders Author Manuscripts

a reduced SRLM integrity in the AD but not in the MCI groups, indicating more pronounced pathological changes in established AD than MCI.

Materials and Methods

Subjects

We studied subjects with MCI (N = 22) and AD (N = 13) from secondary care memory clinics and services in Cambridgeshire and the surrounding area, and aged-matched healthy controls (N = 27) recruited from the healthy partners of the patients and from advertising in the local area. Subjects were classified according to the current clinical diagnostic criteria for AD [18] or MCI [19]. All subjects underwent physical and cognitive assessment with the Mini Mental State Examination (MMSE) [20], Addenbrookes Cognitive Examination Revised (ACE-R) [21] and Rey Auditory Verbal Learning Test (RAVLT) [22]. Written consent was obtained from participants and their informants. Ethical approval for the study protocol was obtained from the National Research Ethics Service – East of England Committee.

MRI Acquisition

All subjects underwent 3T structural MRI at the Cambridge Wolfson Brain Imaging Centre including volumetric T1-weighted (176 slices, 1.0 x 1.0 mm, 1.0 mm slice thickness, TR = 2300ms, TE = 2.98ms, flip angle 9°) and two acquisitions of a high resolution hippocampal, T2-weighted coronal sequence (24 slices, 0.4 x 0.4mm, slice thickness 2.0 mm. TR = 6420ms; TE = 11ms; flip angle 160°) optimized to visualize hippocampal subfields and surrounding brain areas (Firbank et al., 2010). However, the T2 images have partial coverage due to the narrow field of view.

Automated Hippocampal Volume Analysis

Brain tissue segmentation into grey matter (GM), white matter (WM) and cerebrospinal fluid (CSF) was performed using the T1-weighted volumetric images and the Gaussian mixture model in VBM toolbox of SPM8 (http://www.fil.ion.ucl.ac.uk/spm). The GM maps were then normalized using the DARTEL algorithm. Hippocampal region of interests (ROIs) were selected using AAL atlas in MNI space, and then inverse normalized back to each subject's native space using the participant-specific diffeomorphic parameters estimated from the previous DARTEL procedure. The resulting ROIs were also masked using the thresholded GM probability maps (at threshold $p > 0.8$) before the total hippocampal volume was calculated. Finally, in order to control for global volume effects, the hippocampal volumes were normalized by the estimated total intracranial volume (ICV).

Hippocampal Subfields analysis

Hippocampal subfields were segmented manually using the high resolution (0.4mm x 0.4 mm) T2 weighted MRI data. A total of five subjects (1 AD, 2 Control and 2 MCI) were excluded from the analysis due to motion artefact and distortion on the T2 high resolution images. (The scan quality was evaluated visually by raters in brain areas outside the hippocampus regions to avoid circularity in statistical inference). As mentioned previously, in order to increase the signal to noise ratio we acquired two images for each subject and

aligned them before averaging to produce a final image. The amount of head movement between the two acquisitions was estimated using the transformation matrix derived from the linear co-registration process between the two T2 images. We computed the norms from the motion parameters and compared them among the groups in order to assess whether there was systematic bias due to head motion. The averaged images for each subject were then analysed by two raters (L.H. and S.S.), blinded to the diagnosis and subject characteristics, using an established manual approach, in which the subfields CA1, CA2, CA3/DG were segmented on the 3 coronal slices directly posterior to the head of hippocampus [12,14]; see Figure 1. The areas of the traced structures were calculated and retained for subsequent analysis.

The subiculum thickness (Figure 1) was measured at the point immediately before it joins the medial hippocampus on the three slices that had hippocampal traces made. The ERC thickness was measured at the same point on the first slice of the hippocampal tracings and then on the two slices anterior to this (in the hippocampal head) with the line drawn perpendicular to the inferior border of the ERC. Finally, we used a previously validated rating scale for visually scoring the clarity of the hypo intense line representing the SRLM (Figure 2). The values for the subfield area, the ERC and subiculum thickness and the SRLM clarity score were averaged across the left and right hemispheres and the three image slices analysed.

Test-retest Reliability

We assessed the intra-rater reliability of the tracings by repeating the measurements with the same rater one month after the initial tracings. It was performed on a test dataset randomly subsampled 3 subjects from each group. As with the initial tracing, the rater was blinded to the diagnosis when repeating the procedure a month later. For inter-rater reliability, both raters traced the same test dataset of 9 subjects. We measured the percentage difference in measurements and Intraclass Correlation Coefficient (ICC), using a two way random model for absolute agreement of measurements.

Statistics

We used SPSS 22 to test for normality of variables (Shapiro-Wilks test), and for variance (Levene’s test). Normally distributed variables were compared using ANOVA (age and total ICV), non-parametric variables (years of education, MMSE and ACE-R score) were compared using Kruskal-Wallis test. Group comparisons of demographic variables were performed using Mann-Whitney U test. Chi-square test was used to test for sex differences between groups. Group difference in head motion was tested using ANOVA. We tested for between group differences in hippocampal subfields (CA1, CA2, CA3/DG), hippocampal volume, ERC and subiculum thickness and SRLM clarity using three way ANCOVA with age, total ICV and years of education as covariates and controlled for multiple comparisons using Bonferroni correction for seven measurements (hippocampal volume, CA1, CA2, CA3/DG, ERC and subiculum thickness and SRLM clarity) with an adjusted p-value threshold of 0.05/7 = 0.0071. Correlation between subfield and cognitive measures was adjusted for age, total ICV and years of education, and controlled for multiple comparisons using Bonferroni correction.

Results

Subject Characteristics

Subject demographic data is summarised in Table 1. There were no significant differences between groups for gender. In addition to significantly reduced MMSE, ACE-R and RAVLT scores in the AD and MCI groups compared to controls, MCI subjects were older and had fewer years of education. There was no significant group difference in head motion between the two T2 image acquisitions ($p = 0.18$).

Automated hippocampal volumetry

We found a significantly reduced hippocampal volume (Table 2) in AD subjects compared to controls ($p < 0.001$). MCI subjects demonstrated a reduced normalized hippocampal volume compared to controls ($p = 0.002$). MCI subjects although having intermediate atrophy compared to AD and controls, were not different from AD subjects ($p = 0.254$) (Figure 3A). This result remained unchanged after excluding the outlier in the MCI group ($p = 0.152$).

Manual Hippocampal Measurements

The reliability of intra- and inter-rater measurements was comparable to what is found in the literature [12,14], with differences in the CA1, CA2 and CA3/DG areas, SRLM clarity and subiculum and ERC thickness below 20%, which is regarded as a good consistency. The intra-rater reliability was generally better than the inter-rater reliability in terms of both percentage size differences and ICC; see Table 3.

We found a significant atrophy of the CA1 ($p = 0.002$) and subiculum ($p < 0.001$) in the AD and MCI groups compared to controls. The MCI and AD group were not significantly different with respect to either CA1 area or subiculum thickness. We did not detect any group differences in other subfields: CA3/DG and CA2. There were no significant differences with respect to thickness measurements of the ERC.

For the hypo intense line clarity corresponding to the SRLM, we found a significant difference between the AD and MCI as well as AD and controls, with AD subjects having significantly reduced line clarity comparing to both MCI ($p = 0.004$) and controls ($p < 0.001$). There were no significant differences found between the MCI and control groups. Table 2 and Figure 3 summarise the results for both manual and automated segmentation of the hippocampus.

Correlation between MRI and Cognitive Measures

In subjects with AD and MCI, there was a significant correlation between MMSE and the CA3/DG areas (r = 0.571, $p = 0.0015$), and SRLM clarity (r = 0.508, $p = 0.0049$). ACE-R total score correlated with CA1 area (r = 0.502, $p = 0.0065$) and CA3/DG area (r = 0.534, $p = 0.0034$). ACE-R memory sub-score correlated with CA3 area (r = 0.562, $p = 0.0018$) and normalized hippocampal GM volume (r = 0.501, $p = 0.0066$). No other significant correlate was found.

Discussion

The key findings of this study were that: (i) both AD and MCI subjects displayed significant atrophy of CA1, subiculum and whole hippocampus volume compared to similarly aged controls, (ii) SRLM integrity was reduced in the AD group compared with similarly aged controls but not in MCI, suggesting that different subfields maybe affected at different stages of disease progression.

The demonstration of CA1 atrophy in AD is consistent with the other studies utilising manual tracing techniques [12,14], or automated radial distances [10,11]. CA1 atrophy in MCI has also been reported [10,15,16], and it has been shown to correlate with heightened risk of conversion from MCI to AD [15]. Although we did not detect any difference in the degree of atrophy between MCI and AD subjects, others have reported that the CA1 atrophy is less marked in MCI subjects [15]. Our finding of similar degrees of CA1 volume loss and subiculum thinning between AD and MCI groups suggests that although they may be a potential early biomarker for detecting AD at the MCI stage, it may not be a reliable imaging marker or reflect core underlying changes associated with the cognitive and functional transition from MCI to AD.

In a recent feasibility *in vivo* study based on 7T MRI, Boutet et al [23] showed that coronal T2* weighted gradient echo images (0.3mm x 0.3mm) were able to separate hippocampal layers that are richer or poorer in neuronal bodies, in particular SRLM from its surrounding layers in CA and DG. Although at a relatively lower static field strength, our protocol has achieved comparable sensitivity as in 7T, therefore potentially providing a wider applicability in clinical settings where 3T MRI is safer and more readily available. The SRLM located at the transition zone of DG and CA1 subfields is rich in fibers and synapses, which provide intra-hippocampal connectivity between the DG, CA1 and CA3, as well as receiving inputs from the inferior temporal lobe and thalamic nucleus. There is evidence of early involvement of the SRLM in AD with loss of synapses [24,25] as well as a thinning of the SRLM detectable on MRI [23,26], which correlates strongly with memory impairment in AD subjects. This suggests a key role in the progression of AD [27], and possibly a sign of transition from MCI to AD, as supported by our findings. A key pathway with synapses projecting to the SRLM is the perforant pathway of the ERC [28], also affected early in the course of AD, with WM tract disruption detectable on MRI [29] as well as GM atrophy [14].

The observed reduction in SRLM clarity may reflect a combination of pathological factors including neuronal loss, increases in water content, iron deposition, gliosis, demyelination or other changes in tissue microstructure and fiber orientations in SRLM. This may be related to the spread of neurofibrillary tangle and microtubule-associated hyperphosphorylated tau pathology [23,30] involved in hippocampal inputs from ERC, and also wider cortical projections from the hippocampus [31,32] likely playing a key role in the propagation of AD pathology5. SRLM clarity was correlated with global measures of cognition (MMSE) suggesting that the integrity of SRLM, a hub region, may be a strong indicator of cognitive decline in AD. Interestingly, it has been found that the clinical symptoms of AD correlated strongly with synaptic dysfunctions rather than loss of the neurons [33]. Similarly, using the same visual rating scale, Firbank et al14 also showed decreased SRLM clarity when

comparing AD to controls. When this was entered into a predictive model of line clarity in combination with subiculum thickness and whole hippocampal volume, it correctly classified 81% of subjects and the MRI indices derived from high resolution imaging correlated with disease severity. Although the SRLM clarity rating could be confounded by head motion, we did not find any significant group difference in movement between the two image acquisitions. The convergent results suggest that hippocampal subfield measures might indeed reflect disease progression from MCI to AD, although we recognise that our study is cross-sectional and not longitudinal.

Other sub-fields may be pathologically implicated in AD progression, but imaging results are less consistent. For example, Mueller et al (2010), found that the CA1 to CA2 transition zone was the feature most able to discriminate MCI from controls. However, they used the width of the dorsal CA1 region to delineate this CA1-CA2 transition, and thus could in part be a reflection of changes to that area of CA1. We found no correlation between the CA2 area and subject group mostly due to difference in methodology. We also found no significant differences between the CA3/DG regions, in keeping with some previous reports [12,13,14] but not others. For example, Yassa et al [34] reported atrophy in MCI subjects in the CA3/DG region, although this may be explained by the use of T1 weighted images, normalized and mapped to a template which included the CA2 sub-region as part of CA3/DG, and subsequently may not be reflective of the subfield boundaries used in this study.

We also detected no difference in the width of the ERC, known from previous pathological studies to be affected early in AD [5]. Firbank et al [14] using the same technique, identified significant reductions in the thickness of the ERC and subiculum, and this atrophy has been demonstrated by other groups [12,13]. Although we detected a significant reduction in subiculum thickness in AD subjects compared to controls, consistent with the work of others [13,14], we highlight the comparatively poor reliability for ERC and subiculum thickness, emphasizing the difficulties in accurate detection of the subiculum and ERC morphology on *in vivo* MRI images, and for that reason we have interpreted these results with caution. We have previously highlighted the variability that is encountered when measuring these areas (area *versus* length measurement), but even adjusting the technique to encompass width measurements (as per Firbank et al [14]), rather than area or volume measurements, it is still difficult to reliably measure these two regions, or the CA2 total area due to the lack of contrasts and reliable radiological landmarks in separating these structures from their surrounding tissues even at high field strength [17].

There are several limitations to the current study. Although our patient cohorts were recruited according to strict clinical criteria, there has been no histological validation of these clinically probable diagnoses. In addition, our MCI group was older and had fewer years of education than the AD group. Finally, the manual segmentation approach is time consuming and requires extensive training in order to achieve high reliability between raters. In a separate study by our group, hippocampal subfields were segmented using the automated FreeSurfer analysis for the same cohort [35]. In that study, we also found the same pattern of CA1, subiculum and whole hippocampal atrophy as the current study. However, we did not find any significant difference in SRLM between the AD and MCI

groups perhaps due to the lack of sensitivity for FreeSurfer algorithm in quantifying this specific structure.

Conclusion

We have found that CA1 atrophy and subiculum thinning is significantly greater in AD and MCI subjects than controls, but similar between MCI and AD, confirming previous studies indicating that CA1 and subiculum changes occur early in the disease process. Interestingly, only AD participants showed a reduction of SRLM clarity with no AD subjects scoring higher than 3 points, reflecting decreased integrity of the SRLM fiber network. This may be due to later changes associated with the transition from MCI to AD, and represents the wider spread of pathological change associated with the clinical expression of AD dementia [36]. Importantly, the measures of hippocampal subfield atrophy correlated with global cognitive function and memory performance, supporting their potential as biomarkers. Longitudinal imaging studies with our method would be useful to study disease progression and the impact of disease modifying interventions.

Acknowledgment

The study was funded by the National Institute for Health Research (NIHR) Biomedical Research Centre and Biomedical Research Unit in Dementia based at Cambridge University Hospitals NHS Foundation Trust and the University of Cambridge, and Alzheimer's Research UK. We thank the CRN Dementias and Neurodegenerative diseases research network (Eastern) for help with recruitment. J.B.R. is supported by the Wellcome Trust (103838). The views expressed are those of the authors and not necessarily those of the NHS, the NIHR or the Department of Health.

References

[1]. Pennanen C, Kivipelto M, Tuomainen S, Hartikainen P, Haninen T, Laakso MP, Hallikainen M, Vanhanen M, Nissinen A, Helkala EL, Vainioe P, et al. Hippocampus and entorhinal cortex in mild cognitive impairment and early AD. Neurobiol Aging. 2004; 25:303–310. [PubMed: 15123335]

[2]. Jack CR Jr, Peterson RC, O'Brien PC, Tangalos EG. MR-based hippocampal volumetry in the diagnosis of Alzheimer's disease. Neurology. 1992; 42:183–188. [PubMed: 1734300]

[3]. Camicioli R, Moore MM, Kinney A, Corbridge E, Glassberg K, Kaye JA. Parkinson's disease is associated with hippocampal atrophy. Mov Disord. 2003; 18:784–790. [PubMed: 12815657]

[4]. Barber R, Ballard C, McKeith IG, Gholkar A, O'Brien JT. MRI volumetric study of dementia with Lewy bodies: a comparison with AD and vascular dementia. Neurology. 2000; 54:1304–9. [PubMed: 10746602]

[5]. Braak H, Braak E. Neuropathological staging of Alzheimer-related changes. Acta Neuropathologica. 1991; 82(4):239–259. [PubMed: 1759558]

[6]. Liu L, Drouet V, Wu JW, Witter MP, Small SA, Clelland D, Duff K. Trans-synaptic spread of tau pathology in vivo. PloS One. 2012; 7:e31302. [PubMed: 22312444]

[7]. Frost B, Jacks RL, Diamond MI. Propagation of Tau misfolding from the outside to the inside of a cell. J Biol Chem. 2009; 282:12845–12852.

[8]. Ramon y Cajal S. Estructura del asta de Ammon y fascia dentate. Ann Soc Esp Hist Nat. 1893; 22:53–114.

[9]. Jarsky T, Roxin A, Kath WL, Spruston N. Conditional dendritic spike propagation following distal synaptic activation of hippocampal CA1 pyramidal neurons. Nat Neurosci. 2005; 8:1667–1676. [PubMed: 16299501]

Europe PMC Funders Author Manuscripts

Europe PMC Funders Author Manuscripts

[10]. Apostolova LG, Dinov ID, Dutton RA, Hayashi KM, Toga AW, Cummings JL, Thompson PM. 3D comparison of hippocampal atrophy in amnestic mild cognitive impairment and Alzheimer's disease. Brain. 2006a; 129(11):2867–2873. [PubMed: 17018552]

[11]. Frisoni GB, Sabattoli F, Lee AD, Dutton RA, Toga AW, Thompson PM. In vivo neuropathology of the hippocampal formation in AD: A radial mapping MR-based study. NeuroImage. 2006; 32:104–110. [PubMed: 16631382]

[12]. Mueller SG, Stables L, Du AT, Schuff N, Truran D, Cashdollar N, Weiner MW. Measurement of hippocampal subfields and age-related changes with high resolution MRI at 4T. Neurobiol Aging. 2007; 28:719–726. [PubMed: 16713659]

[13]. Mueller SG, Schuff N, Yaffe K, Madison C, Miller B, Weiner MW. Hippocampal Atrophy Patterns in Mild Cognitive Impairment and Alzheimer's Disease. Hum Brain Mapp. 2010 Sep; 31(9):1339–1347. [PubMed: 20839293]

[14]. Firbank MJ, Blamire AM, Teodorczuk A, Teper E, Burton EJ, Mitra D, O'Brien JT. High Resolution Imaging of the Medial Temporal Lobe in Alzheimer's disease and Dementia with Lewy Bodies. Journal of Alzheimer's disease. 2010; 21:1129–1140.

[15]. Apostolova LG, Dutton RA, Dinov ID, Hayashi K, Toga AW, Cummings JL, Thompson PM. Conversion of mild cognitive impairment to Alzheimer disease predicted by hippocampal atrophy maps. Arch Neurol. 2006b; 63:693–699. [PubMed: 16682538]

[16]. Apostolova LG, Mosconi L, Thompson PM, Green AE, Hwang KS, Ramirez A, Mistur R, Tsui WH, de Leon MJ. Subregional hippocampal atrophy predicts Alzheimer's dementia in the cognitively normal. Neurobiol Aging. 2010 Jul; 31(7):1077–1088. [PubMed: 18814937]

[17]. Coras R, Milesi G, Zucca I, Mastropietro A, Scotti A, Figini M, et al. 7T MRI features in control human hippocampus and hippocampal sclerosis: an ex vivo study with histologic correlations. Epilepsia. 2014; 55(12):2003–2016. [PubMed: 25366369]

[18]. McKhann GM, Knopman DS, Chertkow H, Hyman BT, Jack CR Jr, Kawas CH, et al. The diagnosis of dementia due to Alzheimer's disease: recommendations from the National Institute on Aging Alzheimer's Association workgroups on diagnostic guidelines for Alzheimer's disease. Alzheimers Dement. 2011; 7:263–269. [PubMed: 21514250]

[19]. Petersen RC, Morris JC. Mild cognitive impairment as a clinical entity and treatment target. Archives of Neurology. 2005; 62:1160–1163. [PubMed: 16009779]

[20]. Folstein M, Folstein SE, McHugh PR. Mini-Mental State" a Practical Method for Grading the Cognitive State of Patients for the Clinician. Journal of Psychiatric Research. 1975; 12(3):189–198. [PubMed: 1202204]

[21]. Mioshi E, Dawson K, Mitchell J, Arnold R, Hodges JR. The Addenbrooke's Cognitive Examination Revised (ACE-R): a brief cognitive test battery for dementia screening. Int J Geriartr Psychiatry. 2006; 21:1078–1085.

[22]. Schmidt, M. Rey auditory verbal learning test: A handbook. Western Psychological Services; Los Angeles, CA: 1996.

[23]. Boutet C, Chupin M, Lehericy S, Marrakchi-Kacem L, Epelbaum S, Poupon C. Detection of volume loss in hippocampal layers in Alzheimer's disease using 7T MRI: a feasibility study. NeuroImage: Clinical. 2014; 5:341–348. [PubMed: 25161900]

[24]. Lace G, Savva GM, Forster G, de Silva R, Brayne C, Matthews FE, Barclay JJ, Dakin L, Ince PG, Wharton SB, MRC CFAS. Hippocampal tau pathology is related to neuroanatomical connections: an ageing population-based study. Brain. 2009 May; 132(5):1324–34. [PubMed: 19321462]

[25]. Rössler M, Zarski R, Bohl J, Ohm TG. Stage-dependent and sector-specific neuronal loss in hippocampus during Alzheimer's disease. Acta Neuropathologica. 2002; 103(4):363–369. [PubMed: 11904756]

[26]. Kerchner GA, Hess CP, Hammond-Rosenbluth KE, Xu D, Rabinovici GD, Kelley DAC, Vigneron DB, Nelson SJ, Miller BL. Hippocampal CA1 apical neuropil atrophy in mild Alzheimer disease visualized with 7-T MRI. Neurology. 2010; 75:1381–1387. [PubMed: 20938031]

[27]. Kerchner GA, Deutsch GK, Zeineh M, Dougherty RF, Saranathan M, Rutt BK. Hippocampal CA1 apical neuropil atrophy and memory performance in Alzheimer's disease. Neuroimage. 2012 Oct 15; 63(1):194–202. [PubMed: 22766164]

[28]. Insausti, R., Amaral, DG. Hippocampal formation. Atlas of the human brain. Ed 3. London: Elsevier Academic; 2012.

[29]. Kalus P, Slotboom J, Gallinat J, Mahlberg R, Cattapan-Ludewig K, Wiest R, Nyffeler T, Buri C, Federspiel A, Kunz D, Schroth G, et al. Examining the gateway to the limbic system with diffusion tensor imaging: the perforant pathway in dementia. Neuroimage. 2006; 30:713–720. [PubMed: 16337815]

[30]. Chen TF, Chen YF, Cheng TW, Hua MS, Liu HM, Chiu MJ. Executive dysfunction and periventricular diffusion tensor changes in amnesic mild cognitive impairment and early Alzheimer's disease. Hum Brain Mapp. 2009; 30(11):3826–36. [PubMed: 19441023]

[31]. Clerx L, Visser PJ, Verhey F, Aalten P. New MRI markers for Alzheimer's disease: a meta-analysis of diffusion tensor imaging and a comparison with medial temporal lobe measurements. J Alzheimers Dis. 2012; 29(2):405–29. [PubMed: 22330833]

[32]. Rowley J, Fonov V, Wu O, Eskildsen SF, Schoemaker D, Wu L, et al. White matter abnormalities and structural hippocampal disconnections in amnestic mild cognitive impairment and Alzheimer’s disease. PLoS ONE. 2013; 8(9):e74776. [PubMed: 24086371]

[33]. Scheff SW, Price DA, Schmitt FA, DeKosky ST, Mufson EJ. Synaptic alterations in CA1 in mild Alzheimer disease and mild cognitive impairment. Neurology. 2007; 68:1501–1508. [PubMed: 17470753]

[34]. Yassa MA, Stark SM, Bakker A, Albert MS, Gallagher M, Stark CE. High-resolution structural and functional MRI of hippocampal CA3 and dentate gyrus in patients with amnestic mild cognitive impairment. Neuroimage. 2010; 51(3):1242–1252. [PubMed: 20338246]

[35]. Mak E, Gabel S, Su L, Williams GB, Arnold R, Passamonti L, Vázquez Rodríguez P, Surendranathan A, Bevan-Jones WR, Rowe JB, O’Brien JT. Multi-modal MRI investigation of volumetric and microstructural changes in the hippocampus and its subfields in mild cognitive impairment, Alzheimer’s disease, and dementia with Lewy bodies. International Psychogeriatrics. 2017; 29(4):545–555. [PubMed: 28088928]

[36]. Crews L, Masliah E. Molecular mechanisms of neurodegeneration in Alzheimer's disease. Hum Mol Genet. 2010; 19(R1):R12–20. [PubMed: 20413653]

Europe PMC Funders Author Manuscripts

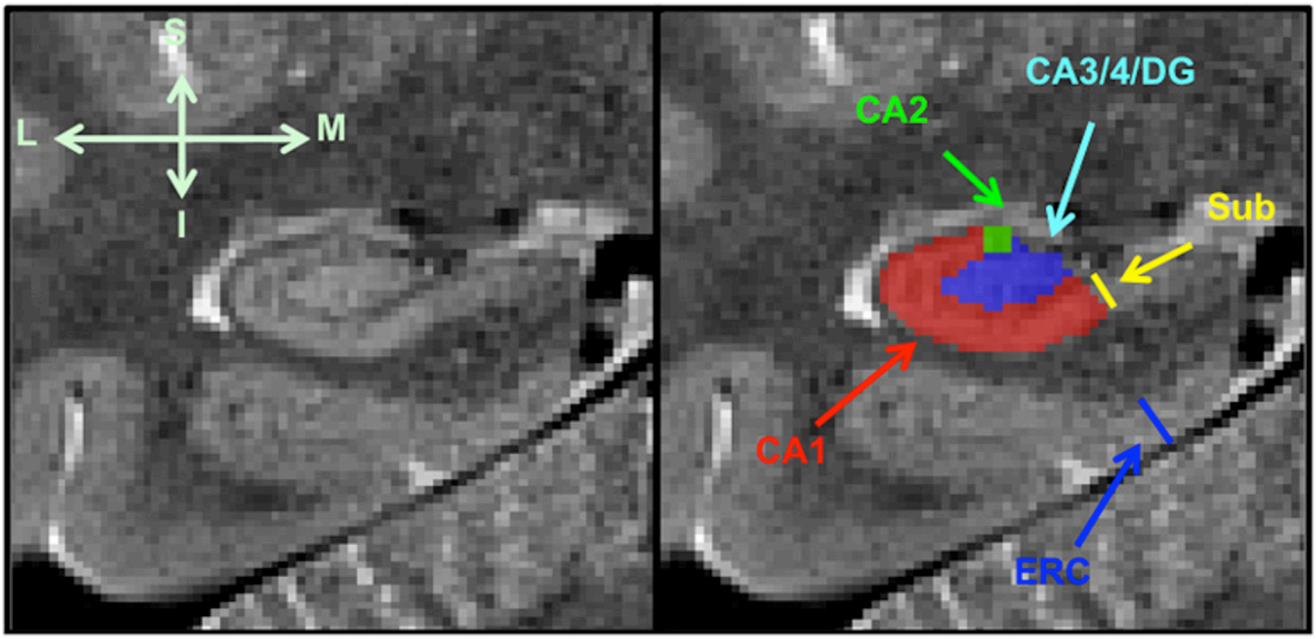

Figure 1. Manual segmentation of the hippocampal subfields

1. Subiculum, delineated at the medial border of the hippocampus, 2. Entorhinal cortex (ERC), measured perpendicular to the inferior border, 3. Cornu Ammonis 1 (CA1) subfield, 4. Cornu Ammonis 3/dentate gyrus (CA3/DG) subfield: the CA1-CA3 boundary is delineated using the clearly visible hypo intense line (left image) 5. Cornu Ammonis 2 (CA2) subfield, marked as the height of the CA1 subfield at the area approximate to the midpoint of horizontal axis

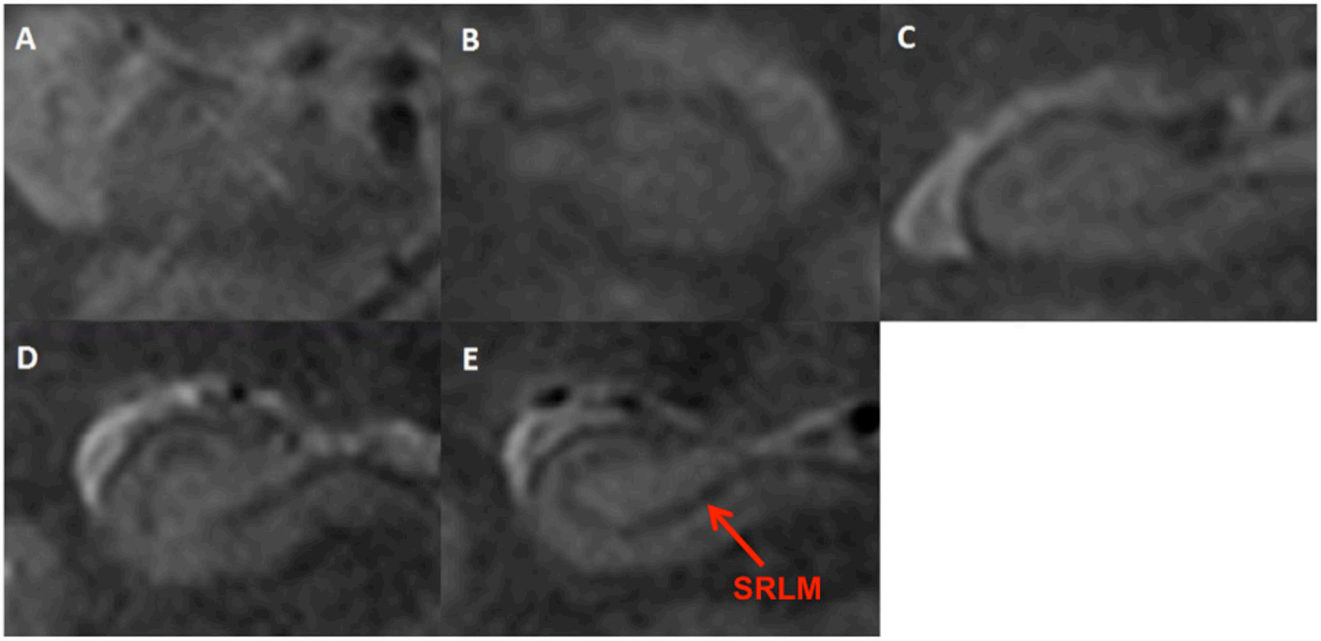

Figure 2. Visual clarity rating

Examples: A. Score 1/5: line is not visible across its entire course, B. Score 2/5: line is visible across less than half its course, C. Score 3/5: line is visible across half of its course, D. Score 4/5: line is visible across over half its course, E. Score 5/5: line is visible across its entire course.

Europe PMC Funders Author Manuscripts

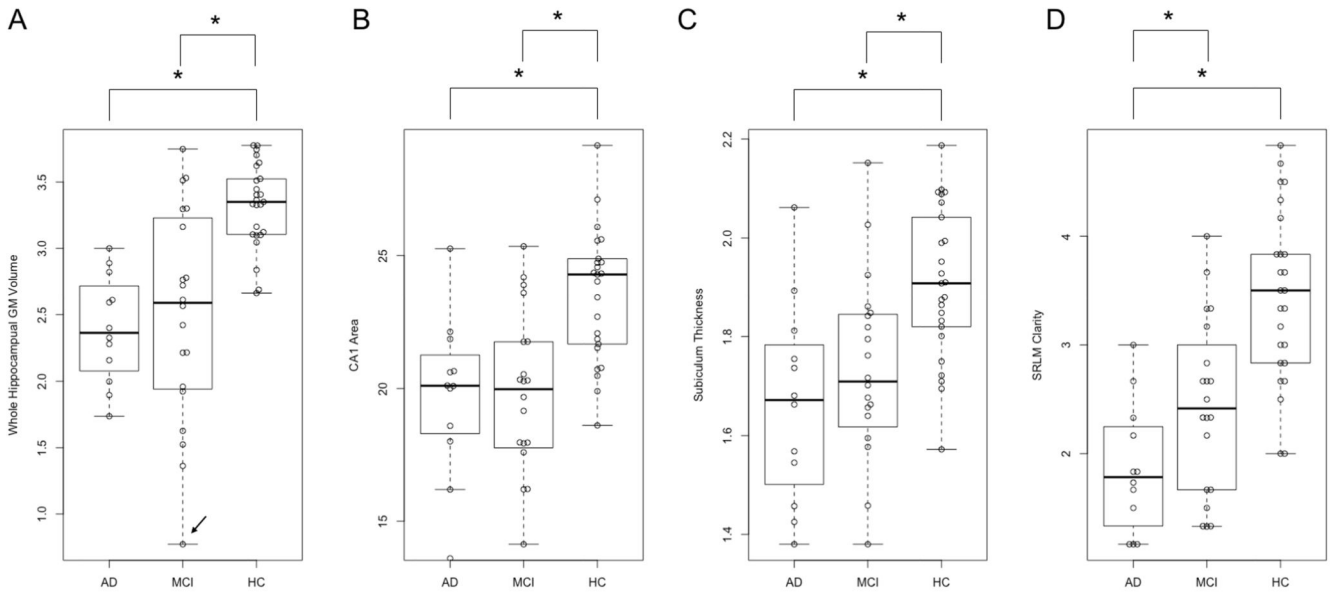

Figure 3. Beeswarm and box plots by group

Significant group differences in A. whole hippocampus GM volume (cm^3), B. CA1 area (mm^2), C. Subiculum thickness (mm), D. SRLM clarity. Note, the outlier in panel A was indicated by an arrow.

Europe PMC Funders Author Manuscripts

Europe PMC Funders Author Manuscripts

Table 1

Demographic, clinical and cognitive characteristics of the three study groups

	Controls (N=25)	MCI (N=20)	AD (N=12)	
Age	66.8 (6.2) [55-80]	75.2 (7.7) [62-90]	67.5 (9.1) [53-84]	$F = 7.78$ $p < 0.001$
Sex (F:M)	13:12	9:11	3:9	$p = 0.3$
Years Education	15.0 (2.7) [10-19]	12.6 (2.7) [10-18]	14.3 (3.4) [10-19]	$X^2 = 6.6$ $p = 0.037$
MMSE	29.0 (1.0) [27-30]	27.3 (1.9) [24-30]	24.3 (3.3) [18-28]	$X^2 = 23.4$ $p < 0.001^{ab}$
ACE-R total	93.1 (5.4) [79-99]	83.7 (7.6) [66-95]	72.6 (11.2) [51-89]	$X^2 = 30.5$ $p < 0.001^{abc}$
ACE-R Memory	23.9 (2.3) [18-26]	17.0 (4.3) [9-24]	13.1 (3.7) [8-20]	$X^2 = 36.5$ $p < 0.001^{ab}$
RAVLT	9.0 (2.7) [3-15]	2.7 (2.7) [0-10]	1.2 (1.3) [0-4]	$X^2 = 34.5$ $p < 0.001^{abc}$
Head movement	0.5 (0.4) [0.04-1.9]	0.6 (0.7) [0.07-2.8]	1.0 (1.2) [0.02-4.3]	*F = 1.79 p = 0.18*

Brackets represent standard deviation (SD) and [Range], F = ANOVA testwise statistic, X^2 = Kruskal-Wallis test statistic.

Abbreviations: MMSE = mini mental state examination, ACE-R = Addenbrookes Cognitive Examination – Revised, RAVLT = Rey Auditory Verbal Learning Test – delayed record score, head movement = norms from the image realignment parameters. Post-hoc analysis (Mann-Whitney U test with Bonferroni correction): a = AD < Control; b = AD < MCI; c = MCI < Controls.

Europe PMC Funders Author Manuscripts

Table 2

Between-group differences in hippocampal measurements

	Controls (N=25)	MCI (N=20)	AD (N=12)	ANCOVA *F p*
CA1 area (mm^2)	23.8 (2.9) [22.6-25.0]	19.5 (3.5) [17.9-21.1]	19.7 (3.0) [17.8-21.6]	$F = 9.69$ $p < 0.001^{ac}$
CA2 area (mm^2)	1.4 (0.2) [1.3-1.4]	1.4 (0.2) [1.3-1.5]	1.4 (0.3) [1.3-1.6]	$F = 0.52$ $p = 0.60$
CA3/DG area (mm^2)	18.0 (2.8) [16.9-19.2]	16.4 (3.3) [14.9-18.0]	16.4 (2.50) [14.9-18.0]	$F = 1.95$ $p = 0.15$
Subiculum thickness (mm)	1.9 (0.2) [1.8-2.0]	1.7 (0.2) [1.6-1.8]	1.7 (0.2) [1.5-1.8]	$F = 11.25$ $p < 0.001^{ac}$
ERC thickness (mm)	2.3 (0.4) [2.2-2.5]	2.3 (0.5) [2.1-2.5]	2.1 (0.2) [2.0-2.3]	$F = 1.45$ $p = 0.24$
SRLM clarity	3.4 (0.8) [3.1-3.8]	2.4 (0.8) [2.1-2.8]	1.9 (0.6) [1.5-2.2]	$F = 16.82$ $p < 0.001^{ab}$
Hippocampal GM Volume (cm^3)	3.3 (0.3) [3.2-3.5]	2.5 (0.8) [2.1-2.9]	2.4 (0.4) [2.1-2.6]	$F = 17.29$ $p < 0.001^{ac}$

Brackets represent standard deviation (SD), [95% confidence interval], F = testwise statistic. ANCOVA adjusted for age, years of education and total intra-cranial volume with Bonferroni correction. Post-hoc analysis: a = AD < Control; b = AD < MCI; c = MCI < Controls.

Europe PMC Funders Author Manuscripts

Table 3

Reliability data

	CA1	CA2	CA3/DG	Subiculum thickness	ERC thickness	SRLM clarity
Inter-rater Reliability						
Percentage difference (%)	11.9	11.7	12.8	11.6	9.2	18.9
ICC (average measures)	0.775	0.798	0.629	0.751	0.572	
Significance *p* value	< 0.001	< 0.001	0.018	< 0.001	0.01	
Weighted kappa value						0.527
Intra-rater Reliability						
Percentage difference (%)	8.3	6.5	9.3	8.3	4.0	12.7
ICC (average measures)	0.83	0.832	0.813	0.839	0.559	
Significance *p* value	< 0.001	0.002	0.005	0.004	0.107	
Weighted kappa value						0.722

Reliability data total 9 samples (3 AD, 3 MCI, 3 Controls), percentage difference and ICC is a two-way random model testing absolute agreement. SRLM clarity reliability was computed using the weighted Cohen's kappa instead of the ICC because SRLM clarity is an ordinal variable.